

# Coherent optical link over hundreds of metres and hundreds of terahertz with subfemtosecond timing jitter

I. CODDINGTON<sup>1</sup>, W. C. SWANN<sup>1</sup>, L. LORINI<sup>2</sup>, J. C. BERGQUIST<sup>1</sup>, Y. LE COQ<sup>3</sup>, C. W. OATES<sup>1</sup>, Q. QURAIHI<sup>1</sup>, K. S. FEDER<sup>4</sup>, J. W. NICHOLSON<sup>4</sup>, P. S. WESTBROOK<sup>4</sup>, S. A. DIDDAMS<sup>1</sup> AND N. R. NEWBURY<sup>1\*</sup>

<sup>1</sup>National Institute of Standards and Technology, 325 Broadway M.S. 815 Boulder, Colorado 80305, USA

<sup>2</sup>Present address: Istituto Nazionale di Ricerca Metrologica INRiM, Strada delle Cacce 91, I-10135 Torino, Italy

<sup>3</sup>Present address: LNE-SYRTE Observatoire de Paris, 61 avenue de l'Observatoire 75014 Paris, France

<sup>4</sup>OFS Laboratories, 19 Schoolhouse Road, Somerset, New Jersey 08873, USA

\*e-mail: nnewbury@boulder.nist.gov

Published online: 1 May 2007; doi:10.1038/nphoton.2007.71

Recent developments in stabilized lasers have resulted in ultrastable optical oscillators with spectral purities below 1 Hz refs 1–6. These oscillators are not transportable at present and operate at a single frequency. To realize their full potential, a highly coherent, frequency-diverse fibre-optic network is needed to faithfully transfer the optical signals to remote sites and to different optical frequencies. Here we demonstrate such a coherent network composed of erbium fibre and Ti:sapphire laser-based, optical-frequency combs<sup>7–9</sup>, stabilized optical-fibre links<sup>4,10</sup> and cavity-stabilized lasers<sup>4–6</sup>. We coherently transmit an optical carrier over 750 m of optical fibre with conversions to wavelengths of 657, 767, 1,126 and 1,535 nm, an overall timing jitter of 590 attoseconds, and a frequency instability of 12 mHz for the 195 THz carrier in 1 s and 250  $\mu$ Hz in 1,000 s. This first remote synchronization of two frequency combs also demonstrates a factor of 30 improvement in the relative stability of fibre frequency combs<sup>11,12</sup>.

In recent years, several groups have used fibre-optic networks for the transfer of stable microwave frequencies over a modulated optical wave<sup>13–18</sup>. Signals have been faithfully transmitted with fractional frequency instabilities of  $5 \times 10^{-15}$  at 1 s over fibre lengths of 86 km and with residual timing jitters of tens of femtoseconds<sup>13,15</sup>. The higher frequencies available with an optical carrier can potentially provide improved resolution, leading to even lower instability and smaller timing jitter by several orders of magnitude<sup>18</sup>. Indeed, this basic fact has driven the strong development of optical clocks, where a laser source is first phase-stabilized to an optical cavity and then ultimately frequency-steered to an atomic transition to provide a phase-coherent, frequency-stable source<sup>19–21</sup>. Using the now ubiquitous fibre-optic network, one can consider transferring the highly coherent optical signal generated by dedicated laboratory systems to remote locations for a variety of applications, including the comparison of different optical clocks to verify their performance and even to search for variations of the fundamental constants<sup>22–24</sup>. Other applications, such as precision spectroscopy, navigation and remote sensing also stand to benefit from the distribution of

highly coherent, stable, low-jitter optical sources. Finally, a highly stable low-phase-noise microwave signal can be generated at the remote end either through the use of a frequency comb<sup>25</sup> or by transmission of dual optical frequencies<sup>17</sup>, albeit with some additional excess jitter.

It is interesting to compare the basic requirements of such a coherent fibre network with those of current telecommunications systems using differential phase-shift keying (DPSK)<sup>26</sup>, which is essentially a coherent network with the different goal of providing high-bandwidth communication. Both networks benefit from the high carrier frequency of the optical wave, an all-optical network, frequency agility to cover the C band and low phase noise. However, for DPSK systems, the required optical-carrier-frequency instability is hundreds of megahertz over approximately millisecond timescales<sup>27</sup>, the required pulse timing jitter is  $\sim 0.5$  ps and a low optical phase noise is needed only on the 100 ps timescales over which the information is transferred. In contrast, for our coherent network to support the high coherence of state-of-the-art optical sources, the required frequency instability is  $< 100$  mHz over approximately second timescales, the required timing jitter is below a femtosecond, and the low optical phase noise should be maintained over minutes or longer. In other words, we wish to preserve the signal character at low Fourier frequencies. This performance should be maintained after transmission down the optical fibre and after wavelength-conversion at network nodes, which can facilitate passive optical wavelength routing as well as provide the desired optical frequency to the user.

The basic components for addressing these challenges include Doppler-cancelled transport over fibre-optic links<sup>4,10</sup>, high-stability, low-phase-noise optical frequency combs<sup>7–9</sup> and well-stabilized lasers<sup>1–6</sup>. Here these components are used in a prototype coherent ring network that can support coherent transfer to any frequency over two octaves of bandwidth, covering both the wavelengths of current optical clocks and the transparent window of the optical fibre. The coherent network has a timing jitter of 590 attoseconds in a bandwidth of 0.06 Hz

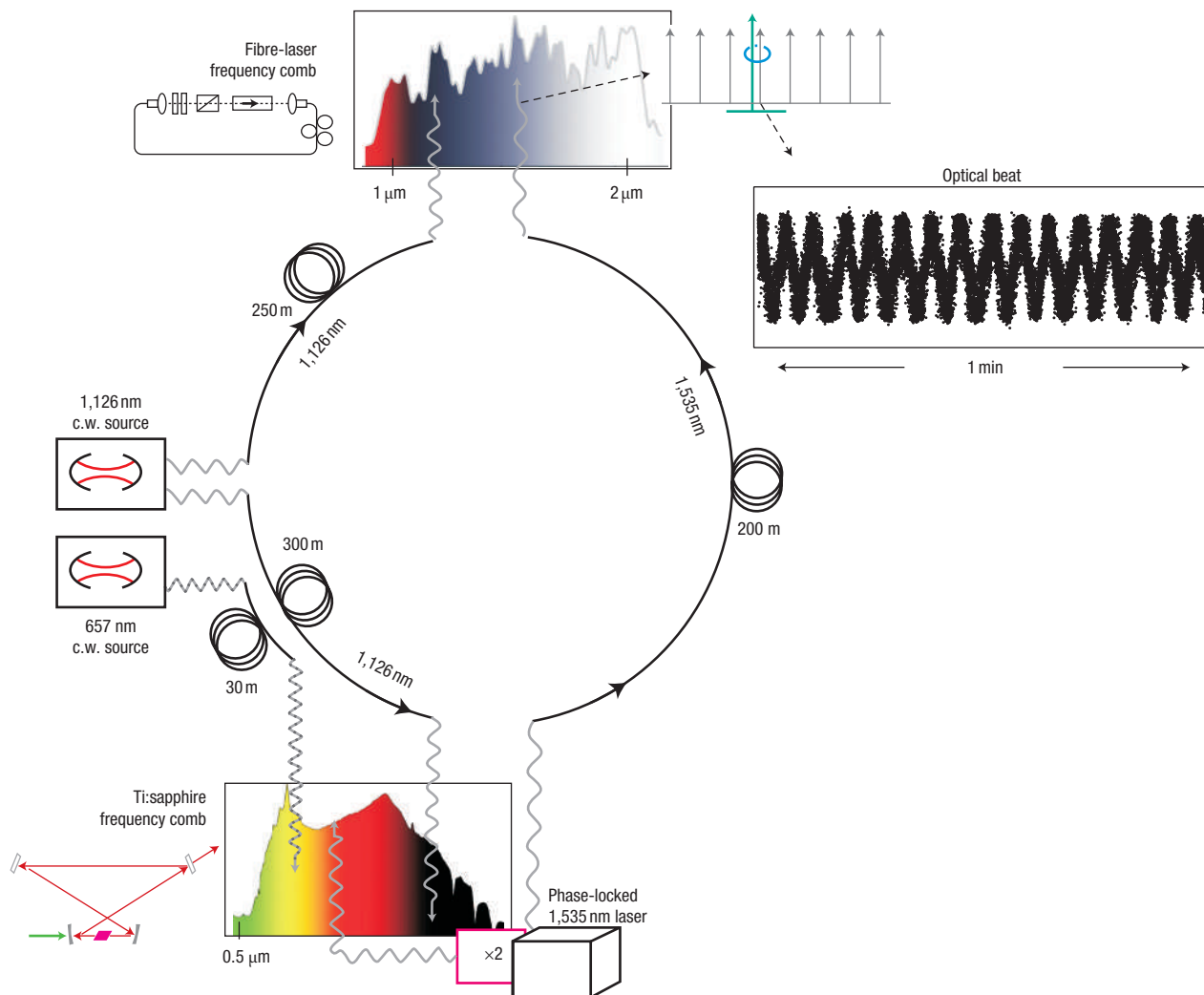


**Figure 1** Schematic of the coherent, frequency-diverse fibre network. Low-jitter optical signals are provided by cavity stabilized lasers at 1,126 nm and 657 nm (left). Two remote frequency combs coherently translate the signals across the spectrum. The first comb (Er-fibre-based) translates the 1,126 nm signal directly to 1,535 nm. The second comb (Ti:sapphire-based) translates either the 1,126 nm or 657 nm signal to 1,535/2 nm. Completing the loop, a c.w. fibre laser at 1,535 nm is doubled, phase-locked to the Ti:sapphire comb and then transmitted to the location of the fibre frequency comb, where its beat note with the 1,535 nm comb tooth is recorded. The inset shows the measured open-loop heterodyne beat note of the two 1,535 nm (195 THz) signals, mixed down to 0.23 Hz (500 samples per second and a 2 MHz input bandwidth). The coherent sine wave so generated is evidence that the transmission and frequency translation around the coherent loop introduced negligible timing jitter or frequency instabilities. The noise on the sine wave is consistent with phase noise of  $\sim 0.6$  rad r.m.s. (see Fig. 2c).

to 25 MHz, and a fractional frequency instability of  $\langle \delta\nu/\nu \rangle_\tau \approx 6.2 \times 10^{-17} \tau^{-1/2}$ , where  $\tau$  is the averaging time in seconds, which corresponds to  $\delta\nu = 12$  mHz in 1 s for a 195 THz carrier (1,550 nm). The weighted average of different runs totalling five hours gives a frequency fidelity around the network of  $56 \pm 103$   $\mu$ Hz, or  $(2.9 \pm 5.3) \times 10^{-19}$  of the 195 THz carrier.

Figure 1 depicts our prototype coherent network. A highly coherent signal at 1,126 nm is sent through a Doppler-cancelled fibre-optic link<sup>4,10</sup> to a fibre frequency comb with a 50-MHz comb spacing<sup>8,28</sup> (clockwise in Fig. 1). The comb tooth near 1,126 nm is enhanced by  $\sim 5$  dB by a Bragg grating in the nonlinear fibre<sup>29</sup> that spectrally broadens the comb output and phase-locked to the incoming 1,126 nm signal. This phase lock, in conjunction with the self-referenced phase lock of the comb offset frequency, effectively transfers the coherence of the incoming 1,126 nm light to each comb tooth from 1 to 2  $\mu$ m<sup>8,9,30</sup>. Simultaneously, either

that same 1,126 nm source, or an independent 657 nm source, is transmitted through a Doppler-cancelled link to a Ti:sapphire frequency comb<sup>9</sup>, which spans from 550 nm to 1.2  $\mu$ m (counterclockwise in Fig. 1) with a 1-GHz comb spacing. By again locking one tooth of this comb to one or the other source, the source coherence is transferred to each comb tooth. A 1,535 nm continuous-wave (c.w.) fibre laser is co-located with the Ti:sapphire frequency comb. The output of the c.w. fibre laser is amplified to 500 mW, doubled in periodically poled lithium niobate, and then phase-locked to the Ti:sapphire comb tooth at  $\sim 767.5$  nm. About 1 mW of the fundamental c.w. 1,535 nm light is then transmitted through a third Doppler-cancelled link to the fibre frequency comb, where the open-loop beat signal at 1,535 nm provides a test of the stability, coherence and accuracy preserved by the network through the multiple frequency translations and fibre transmissions.

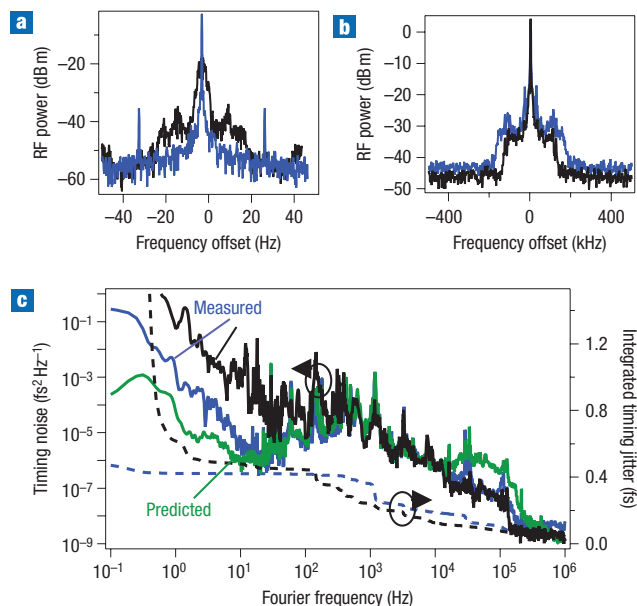


**Figure 2** The heterodyne signal between the two independently generated 1,535 nm signals around the network. **a**, Beat note for a common 1,126 nm source (blue line) or for separate 1,126 nm and 657 nm sources (black line) for a 0.3 Hz RBW. **b**, Expanded range at 3 kHz RBW. The phase-noise pedestal contains  $\sim 25\%$  of the total power. **c**, The timing-jitter spectral density for the beat note with a single common 1,126 nm source (blue line) and separate 1,126 nm and 657 nm sources (black line), and the predicted timing jitter (green line) from the measured in-loop noise on the various phase locks. The filled arrows indicate the appropriate y axis for the indicated data. The servo bump at 100 kHz apparent in **b** and **c** depends on the settings of the various phase locks. The timing jitter (dashed lines, right-hand scale) reaches 490 attoseconds integrated from 0.06 Hz to 1 MHz for a common 1,126 nm source (black dashed line), corresponding to 0.6 rad phase jitter. Extrapolation of the measured white-phase-noise floor to 25 MHz (the Nyquist frequency of the fibre frequency comb) gives a projected timing jitter of 590 attoseconds.

As shown in Fig. 1, a coherent sine wave is generated from the mixed-down heterodyne signal between the two 1,535 nm (195 THz) optical signals. The corresponding radio-frequency (RF) spectrum of the heterodyne beat is shown in Fig. 2a with a resolution bandwidth (RBW) of 0.3 Hz and 3 kHz. The full-width half-maximum linewidth is 3 Hz over 2 min if the Ti:sapphire comb is phase-locked to the 657 nm source (after removing relative linear cavity drift) and instrument-limited at 0.1 Hz if it is phase-locked to the common 1,126 nm source. The ‘fuzz’ on the sine wave (Fig. 1) or its Fourier transform, the pedestal on the RF beat note (Fig. 2b), is a result of the timing jitter incurred in the various frequency conversions and transport around the ring. (Under ideal frequency conversion, the timing jitter,  $\Delta t$ , is independent of the carrier frequency,  $\nu$ , unlike the phase jitter,  $\Delta\phi = 2\pi\nu\Delta t$ .) The measured timing-jitter power spectral density versus Fourier frequency is shown in Fig. 2c. The measured jitter compares well with the predicted jitter calculated from the sum of the contributing phase locks around the network down to low Fourier frequencies (see Methods). The dominant contribution to the in-loop jitter arises from the optical phase-locks of the frequency combs, with a  $\sim 0.10$ -fs contribution from phase-locks for Doppler cancellation of the fibre noise. If a common 1,126 nm source is used, the measured timing jitter diverges from the expected jitter below  $\sim 10$  Hz,

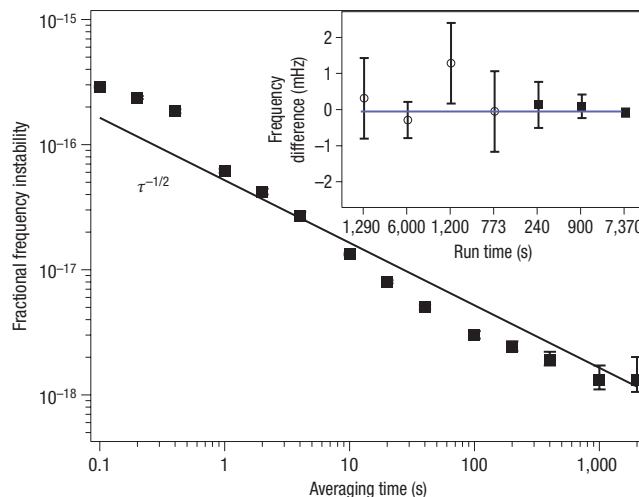


**Figure 3** Fractional frequency uncertainty (total Allan deviation) of the 1,535 nm beat signal versus averaging time  $\tau$  for a common 1,126 nm source. Also shown is a fit with a  $\tau^{-1/2}$  slope. Inset: Difference between the expected and measured frequency versus run time. The average value (blue line) is  $-56 \pm 103 \mu\text{Hz}$ , or only  $(2.9 \pm 5.3) \times 10^{-19}$  from the expected value. The last three runs (filled squares) provided the data for calculating the Allan deviation seen in the main plot. The first four runs (open circles) exhibited a  $\sim \times 2.5$  higher Allan deviation (not shown) because of excess out-of-loop fibre in the phase-lock of the doubled c.w. fibre laser to the Ti:sapphire comb. Plotted error bars are simply the Allan deviation for that data set evaluated at the run time.

presumably due to drifts in the cumulative few metres of fibre and air paths around the network that are ‘out-of-loop’ (that is, not encompassed within the phase locks associated with either the frequency combs or the Doppler-cancelled fibre links). Indeed ‘ $1/f$ ’ temperature fluctuations of  $\sim 0.6 \text{ mK Hz}^{-1/2}$  at 1 Hz over  $\sim 1$  m of silica fibre would yield the observed low-frequency timing jitter. If both the 657 nm and 1,126 nm sources are used, the measured timing jitter diverges from the expected jitter below  $\sim 50$  Hz due to drifts between the two coherent sources.

The fractional frequency instability of the heterodyne beat signal at 1,535 nm is expressed by the Allan deviation  $\langle \delta\nu/\nu \rangle_\tau$  as a function of averaging time  $\tau$  in seconds and is shown in Fig. 3. The measured value of  $\langle \delta\nu/\nu \rangle_{1\text{s}} = 6.2 \times 10^{-17}$  or  $\langle \delta\nu/\nu \rangle_{1,000\text{s}} = 1.3 \times 10^{-18}$  and is consistent with previous measurements of the Ti:sapphire frequency comb<sup>30</sup>, demonstrating that our fibre-laser frequency comb can provide performance comparable to Ti:sapphire-based systems. It is also consistent with the instability expected from the low-frequency timing jitter, which is likewise attributed to environmentally induced variations in the out-of-loop path lengths<sup>30</sup>. The slope of the Allan deviation roughly agrees with that expected from white frequency noise (that is,  $\tau^{-1/2}$ ). The inset of Fig. 3 plots the difference between the measured value of the beat frequency and the expected value, calculated from the frequency scalings and shifts incurred around the loop (see Methods). The average offset is  $56 \pm 103 \mu\text{Hz}$  from the expected value, giving a fractional offset of  $(2.9 \pm 5.3) \times 10^{-19}$ .

The extension of the network to multiple transmitted wavelengths and longer transmission distances will be required to exploit fully the next generation of optical sources. For example, multiple transmitters at different wavelengths in the C band could be phase-locked to either comb and transmitted over

Doppler-cancelled fibre links with signal routing provided by passive optical components. Preliminary measurements indicate links longer than 50 km are achievable before the timing jitter from the fibre link becomes comparable to that of the frequency combs (that is, the 1-fs level), at which point one could use coherent repeaters<sup>18</sup>. The overall performance demonstrated here shows that the various technologies of phase-stabilized c.w. lasers, frequency combs and fibre links can be successfully incorporated into a fibre network capable of preserving the stability and phase noise of current optical sources while bridging large distances and traversing the optical spectrum.

METHODS

The performance of the network was evaluated through the heterodyne beat signal at the location of the fibre frequency comb. This heterodyne signal arises from mixing the coherent 1,535 nm signal delivered through one path of the loop (clockwise in Fig. 1) with the signal that travelled along the second path of the loop (counterclockwise in Fig. 1). As the coherent signal travels around the ring, it is both scaled in frequency through the use of frequency combs and shifted in frequency, for example, through the action of acousto-optic modulators (AOMs). Each of these translations or scalings is connected with a phase-locked loop that phase-locks the frequency of the heterodyne beat signal to an RF oscillator. For example, cancellation of Doppler shifts due to fibre-path-length fluctuations is accomplished by retro-reflecting a signal from the fibre's end, heterodyning this signal with the source light and phase-locking the resulting beat signal to an RF oscillator by feeding back to an in-line AOM<sup>4,10</sup>. Similarly, the entire frequency comb is phase-locked by phase-locking both the carrier-envelope offset (CEO) frequency and the frequency of the heterodyne beat between a single comb tooth and a stabilized optical source at either 1,126 nm or 657 nm to an RF source<sup>8,9</sup>. With proper book-keeping, we can write expressions for the expected optical frequency generated in each direction around the loop. These expressions are useful in determining the expected value of the beat frequency, the overall instability and the overall timing jitter.

From the standard expressions for the frequency comb<sup>7–9,28,30</sup>, and after some algebra, the frequency of the comb tooth of the fibre-laser frequency comb used to compare the two network arms at 1,535 nm after travelling clockwise (clw) around the ring is

$$\nu_{1,535}^{clw} = r_{Er} \nu_{1,126} + \Delta \nu_{1,535}^{clw} \tag{1}$$

The original 1,126 nm light ( $\nu_{1,126}$ ) is scaled by the factor of  $r_{Er} = n_{Er}(1,535)/n_{Er}(1,126)$ , where  $n_{Er}(\lambda)$  is the mode number of the comb tooth near  $\lambda$ , and then offset by an amount  $\Delta \nu_{1,535}^{clw} = (1 - r_{Er})\nu_{Er,CEO} - r_{Er}(\nu_{Er,opt} - \nu_{Er,AOM})$ , where  $\nu_{Er,CEO}$  is the CEO frequency of the self-referenced erbium-doped fibre-laser frequency comb,  $\nu_{Er,opt}$  is the offset frequency used in phase-locking the fibre frequency comb to the 1,126 nm light, and  $\nu_{Er,AOM}$  is the frequency shift from the AOM used in the Doppler-stabilized fibre link transmitting the 1,126 nm light to the erbium-fibre frequency comb, all of which are constant because they are phase-locked to an RF source. Similarly, travelling counterclockwise (cclw) around the loop in Fig. 1, the frequency of the 1,535 nm signal that arrives at the location of the fibre frequency comb from the c.w. fibre laser is

$$\nu_{1,535}^{cclw} = r_{Ts} \nu_{1,126} + \Delta \nu_{1,535}^{cclw} \tag{2}$$

The original 1,126 nm light is scaled by the factor of  $r_{Ts} = n_{Ts}(767)/2n_{Ts}(1,126)$ , where  $n_{Ts}(\lambda)$  is the mode number of the comb tooth near  $\lambda$  and the factor of 2 arises from the second-harmonic generation used in phase-locking the doubled c.w. fibre laser at 1,535 nm to the comb tooth at 767 nm. The frequency is offset by an amount  $\Delta \nu_{1,535}^{cclw} = (1/2 - r_{Ts})\nu_{Ts,CEO} - r_{Ts}(\nu_{Ts,opt} - \nu_{Ts,AOM}) + \nu_{fl,AOM} + \nu_{fl,Ts}/2$ , where the notation is analogous to that for the erbium-fibre frequency comb,  $\nu_{fl,Ts}$  is the frequency offset between the doubled light from the 1,535-nm c.w. fibre laser and the Ti:sapphire comb tooth at  $n_{Ts}(767)$ , and  $\nu_{fl,AOM}$  is the frequency shift from the AOM used in the Doppler-stabilized fibre link transmitting the 1,535 nm light of the c.w. fibre laser to the erbium-fibre comb.

The difference between equations (1) and (2) is the expected value of the beat frequency  $\nu_{1,535}^{clw} - \nu_{1,535}^{cclw}$ . If the repetition frequencies (that is, mode spacing) of the two combs are commensurate and all the offset frequencies are

carefully chosen, then it can be arranged so that  $r_{Ts} = r_{Er}$  and  $\Delta \nu_{1,535}^{clw} = \Delta \nu_{1,535}^{cclw}$  and therefore  $\nu_{1,535}^{clw} = \nu_{1,535}^{cclw}$  for any 'input' frequency,  $\nu_{1,126}$ . However, the combs will in general have very different repetition frequencies, as is the case here. For our experiment,  $r_{Ts} = 390,180/531,776$ ,  $r_{Er} = 3,894,992/5,308,470 \approx r_{Ts}$ ,  $\Delta \nu_{1,535}^{clw} \approx 38.4$  MHz and  $\Delta \nu_{1,535}^{cclw} \approx 363.10$  MHz. Drifts in the frequency of the 1,126 nm source are suppressed by a factor of  $(r_{Ts} - r_{Er})$ . Using the exact values for the frequency offsets and measured value of  $\nu_{1,126}$ , we find  $\nu_{1,535}^{clw} = 195,304,991,286,408.817246$  Hz and  $\nu_{1,535}^{cclw} = 195,304,897,206,157.425436$  Hz, relative to our H-maser timebase reference, so that  $\nu_{1,535}^{clw} - \nu_{1,535}^{cclw} = 94,080,251.391810$  Hz for the longest two-hour run. This value differs from the measured value by 86  $\mu$ Hz, giving a fractional frequency offset of  $86 \mu\text{Hz}/195 \text{ THz} = 4.4 \times 10^{-19}$ , as shown as the last point in the inset of Fig. 3 (the average offset over all runs is 56  $\mu$ Hz). Clearly, this level of accuracy requires the various RF frequencies to be known to better than  $\sim 100 \mu$ Hz; in our case, this condition is assured, because all RF oscillators were phase-locked to a single hydrogen maser. However, a compact GPS-steered Rb oscillator can provide an uncertainty of  $1 \times 10^{-12}$ ; assuming the RF frequency offsets are chosen to be on the  $\sim 100$  MHz level, the relative optical frequency can be determined to  $10^{-12} \times 100 \text{ MHz}/195 \text{ THz} = 5 \times 10^{-19}$ . In a similar vein, instability of  $6 \times 10^{-17}$  at a second for the optical signals requires an instability of the local RF source of  $(195 \text{ THz}/100 \text{ MHz}) \times (6 \times 10^{-17}) = 10^{-10}$  at one second, easily met by a quartz oscillator. In summary, because any instability of the RF source adds to that of the optical source, there is a factor of  $\sim (100 \text{ MHz}/195 \text{ THz})$  suppression in terms of its effect on the optical signal instability.

Equations (1) and (2) are also useful in predicting the accumulated timing jitter around the loop. Each of the RF frequencies that contributes to the shifts  $\Delta \nu_{1,535}^{clw}$  and  $\Delta \nu_{1,535}^{cclw}$  in equations (1) and (2) is associated with a phase-lock of the frequency of the relevant heterodyne beat signal to an RF source. These phase-locks will not be perfectly tight, and therefore phase jitter will accumulate as the signal travels around the network, ultimately manifesting itself as phase noise or timing noise on the beat signal  $\nu_{1,535}^{clw} - \nu_{1,535}^{cclw}$ , which is typically quantified in terms of the power spectral density (PSD). (The intrinsic jitter of a laboratory RF source is typically negligible in comparison to the jitter in the phase-lock.) The book-keeping is considerably simplified if we consider the timing PSD rather than phase PSD, related by  $S = (2\pi\nu\lambda)^{-2} S_\phi$ , where  $S$  is the timing PSD,  $S_\phi$  is the phase PSD and  $\nu\lambda = c/\lambda$  is the relevant optical carrier frequency. The predicted overall timing jitter PSD on the optical beat signal at 1,535 nm (195 THz) from equations (1) and (2) is

$$S_{\text{beat}} = S_{Er,opt} + S_{Ts,opt} + S_{Ts,AOM} + S_{Er,AOM} + S_{fl,AOM} + S_{fl,Ts} + a_{Er}^2 S_{Er,CEO} + a_{Ts}^2 S_{Ts,CEO} \tag{3}$$

where the timing jitter of the fibre-link phase-lock  $S_{fl,AOM}$  is calculated using a carrier frequency at 1,535 nm, the timing jitter of the c.w. fibre laser optical lock  $S_{fl,Ts}$  is calculated using a carrier frequency at 767.5 nm, and the timing jitter of the CEO phase lock  $S_{Er(Ts),CEO}$ , the optical phase-locks  $S_{Er(Ts),opt}$  and the fibre-link phase-locks  $S_{Er(Ts),AOM}$  are calculated using a carrier frequency at 1,126 nm.  $a_{Er} = 1 - r_{Er}^{-1}$ ,  $a_{Ts} = 1 - (2r_{Ts})^{-1}$  and we have dropped the cross-correlation terms between  $S_{Er(Ts),opt}$  and  $S_{Er(Ts),CEO}$  (ref. 28). All the PSDs on the right-hand side are measured from the in-loop error signal. The sum  $S_{\text{beat}}$  is plotted in Fig. 2c and is dominated by the first two terms. As discussed in the text, at low Fourier frequencies, there is excess timing-jitter noise not included in equation (3) that is presumed to arise from out-of-loop fibre and air paths.

In addition to the noise, there will be occasional cycle slips where a phase-lock temporarily loses lock, corresponding to an unknown jump in the timing of one of the optical signals. If properly removed, the effect of these slips is only to reduce the effective averaging time without biasing the measurement. To monitor for cycle slips, the frequency of the RF signals for each phase-lock was counted during the measurement. A cycle slip on any one of the phase locks was readily seen as a change in the counted signal by  $1/t_{\text{gate}}$  from the phase-locked value, where  $t_{\text{gate}}$  is the counter gate time. The data contributing to the Allan deviation in Fig. 3 includes only those times when no such cycle slips were measured. As the phase-locks were improved, these cycle slips became much less frequent; for the longest two-hour run there were no cycle slips on either the offset frequency or optical frequency lock of the fibre frequency comb. If undisturbed, both combs now operate for hours without cycle slips.

Received 19 January 2007; accepted 19 March 2007; published 1 May 2007.

## References

1. Stoehr, H., Mensing, F., Helmcke, J. & Sterr, U. Diode laser with 1 Hz linewidth. *Opt. Lett.* **31**, 736–738 (2006).
2. Webster, S. A., Oxborrow, M. & Gill, P. Subhertz-linewidth Nd:YAG laser. *Opt. Lett.* **29**, 1497–1499 (2004).
3. Notcutt, M., Ma, L.-S., Ye, J. & Hall, J. L. Simple and compact 1-Hz laser system via an improved mounting configuration of a reference cavity. *Opt. Lett.* **30**, 1815–1817 (2005).
4. Young, B. C., Cruz, F. C., Itano, W. M. & Bergquist, J. C. in *Laser Spectroscopy (XIV International Conference)* (eds Blatt, R., Eschner, J., Leibfried, D. & Schmidt-Kaler, E.) 61–70 (World Scientific, Singapore, 1999).
5. Young, B. C., Cruz, F. C., Itano, W. M. & Bergquist, J. C. Visible lasers with subhertz linewidths. *Phys. Rev. Lett.* **82**, 3799–3802 (1999).
6. Oates, C. W., Curtis, E. A. & Hollberg, L. Improved short-term stability of optical frequency standards: approaching 1 Hz in 1 s with the Ca standard at 657 nm. *Opt. Lett.* **25**, 1603–1605 (2000).
7. Udem, T., Holzwarth, R. & Hänsch, T. W. Optical frequency metrology. *Nature* **416**, 233–237 (2002).
8. Swann, W. C. *et al.* Fiber-laser frequency combs with sub-hertz relative linewidths. *Opt. Lett.* **31**, 3046–3048 (2006).
9. Fortier, T. M., Bartels, A. & Diddams, S. A. Octave-spanning Ti:sapphire laser with a repetition rate >1 GHz for optical frequency measurements and comparisons. *Opt. Lett.* **31**, 1011–1013 (2006).
10. Ma, L. S., Jungner, P., Ye, J. & Hall, J. L. Delivering the same optical frequency at two places: Accurate cancellation of phase noise introduced by an optical fiber or other time-varying path. *Opt. Lett.* **19**, 1777–1779 (1994).
11. Schnatz, H., Lipphardt, B. & Grosche, G. in *Conference on Lasers and Electro-Optics/Quantum Electronics and Laser Science Conference (CLEO) 2006 Technical Digest CTuH1* (Optical Society of America, Long Beach, California, 2006).
12. Kubina, P. *et al.* Long term comparison of two fiber based frequency comb systems. *Opt. Express* **13**, 904–909 (2005).
13. Lopez, O. *et al.* in *2006 IEEE International Frequency Control Symposium and Exposition 80–82* (IEEE, Miami, Florida, 2006).
14. Daussy, C. *et al.* Long-distance frequency dissemination with a resolution of  $10^{-17}$ . *Phys. Rev. Lett.* **94**, 203904 (2005).
15. Hudson, D., Foreman, S. M., Cundiff, S. T. & Ye, J. Synchronization of mode-locked femtosecond lasers through a fiber link. *Opt. Lett.* **31**, 1951–1953 (2006).
16. Musha, M. *et al.* Robust and precise length stabilization of a 25-km long optical fiber using an optical interferometric method with a digital phase-frequency discriminator. *Appl. Phys. B* **82**, 555–559 (2006).
17. Shillue, B. in *LEOS Summer Topical Meeting on Optical Frequency & Time Measurement and Generation TuB4.2* (San Diego, California, 2005).
18. Ye, J. *et al.* Delivery of high-stability optical and microwave frequency standards over an optical fiber network. *J. Opt. Soc. Am. B* **20**, 1459–1467 (2003).
19. Oskay, W. H. *et al.* Single-atom optical clock with high accuracy. *Phys. Rev. Lett.* **97**, 020801 (2006).
20. Gill, P. Optical frequency standards. *Metrologia* **42**, S125–S137 (2005).
21. Takamoto, M., Hong, F.-L., Higashi, R. & Katori, H. An optical lattice clock. *Nature* **435**, 321–324 (2005).
22. Fischer, M. *et al.* New limits on the drift of fundamental constants from laboratory measurements. *Phys. Rev. Lett.* **92**, 230802 (2004).
23. Peik, E. *et al.* Limit on the present temporal variation of the fine structure constant. *Phys. Rev. Lett.* **93**, 170801 (2004).
24. Bize, S. *et al.* Testing the stability of fundamental constants with the Hg-199(+) single-ion optical clock. *Phys. Rev. Lett.* **90**, 150802 (2003).
25. McFerran, J. J. *et al.* Low-noise synthesis of microwave signals from an optical source. *Electron. Lett.* **41**, 650–651 (2005).
26. Gnauck, A. H. & Winzer, P. J. Optical phase-shift-keyed transmission. *J. Lightwave Technol.* **23**, 115–130 (2005).
27. Kim, H. & Winzer, P. J. Robustness to laser frequency offset in direct-detection DPSK and DQPSK systems. *J. Lightwave Technol.* **21**, 1887–1891 (2003).
28. Newbury, N. R. & Swann, W. C. Low-noise fiber-laser frequency combs. *J. Opt. Soc. Am. B* advance online publication, 30 January 2007 (doc. ID: 76696).
29. Westbrook, P. S., Nicholson, J. W., Feder, K. S., Li, Y. & Brown, T. Supercontinuum generation in a fiber grating. *Appl. Phys. Lett.* **85**, 4600–4602 (2004).
30. Ma, L.-S. *et al.* Optical frequency synthesis and comparison with uncertainty at the  $10^{-19}$  level. *Science* **303**, 1843–1845 (2004).

## Acknowledgements

We acknowledge assistance from J. Stalnaker and T. Fortier with the Ti:sapphire frequency comb and useful discussions with L. Hollberg and T. Rosenband. We acknowledge funding from the National Institute of Standards and Technology and from the DARPA PHOR-FRONT program. Correspondence and requests for materials should be addressed to N.N.

## Author contributions

I.C. and W.C.S. were responsible for the c.w.-fibre-laser stabilization and associated fibre link, L.L. and J.C.B. for the stabilized 1,126 nm source and associated fibre links, Y.LeC. and C.W.O. for the stabilized 657 nm source and associated fibre link. S.A.D. and Q.Q. for Ti:sapphire frequency comb, W.C.S. and N.R.N. for the fibre frequency comb, and K.S.F., J.W.N. and P.S.W. for the nonlinear fibre and fibre grating used with the fibre comb. I.C. and N.R.N. analysed the data. S.A.D. and N.R.N. designed the experiment.

## Competing financial interests

The authors declare that they have no competing financial interests.

Reprints and permission information is available online at <http://npg.nature.com/reprintsandpermissions/>